Skeletal Radiology (2021) 50:1557–1565
https://doi.org/10.1007/s00256-020-03689-1

SCIENTIFIC ARTICLE

Morphology of the entering and exiting nerve as a differentiating feature of benign from malignant peripheral nerve sheath tumours of the brachial plexus

I. Pressney[1] · M. Khoo[1] · R. Khan[2] · P. Abernethy[3] · R. Hargunani[1] · A. Saifuddin[1]

Received: 31 August 2020 / Revised: 28 November 2020 / Accepted: 29 November 2020 / Published online: 7 January 2021

Abstract

Objective To identify if morphology of the entering and exiting nerve involved by a nerve sheath tumour in the brachial plexus can help differentiate between benign (B) and malignant (M) peripheral nerve sheath tumours (PNSTs).

Materials and methods Retrospective review of 85 patients with histologically confirmed primary PNSTs of the brachial plexus over a 12.5-year period. Clinical data and all available MRI studies were independently evaluated by 2 consultant musculoskeletal radiologists blinded to the final histopathological diagnosis assessing for maximal lesion dimension, visibility and morphology of the entering and exiting nerve, and other well-documented features of PNSTs.

Results The study included 47 males and 38 females with mean age 46.7 years (range, 8–81 years). There were 73 BPNSTs and 12 MPNSTs. The entering nerve was not identified in 5 (7%), was normal in 17 (23%), was tapered in 38 (52%) and showed lobular enlargement in 13 (18%) BPNSTs compared with 0 (0%), 0 (0%), 2 (17%) and 10 (83%) MPNSTs respectively. The exiting nerve was not identified in 5 (7%), was normal in 20 (27%), was tapered in 42 (58%) and showed lobular enlargement in 6 (8%) BPNSTs compared with 4 (33%), 0 (0%), 2 (17%) and 6 (50%) MPNSTs respectively. Increasing tumour size, entering and exiting nerve morphology and suspected MRI diagnosis were statistically significant differentiators between BPNST and MPNST ($p < 0.001$). IOC for nerve status was poor to fair but improved to good if normal/tapered appearance were considered together with improved specificity of 81–91% for BPNST and sensitivity of 75–83%.

Conclusions Morphology of the adjacent nerve is a useful additional MRI feature for distinguishing BPNST from MPNST of the brachial plexus.

Keywords Schwannoma · Neurofibroma · Malignant peripheral nerve sheath tumour · Neurofibromatosis · NF-1 · Magnetic resonance imaging

Introduction

Tumours of the brachial plexus may be either of primary neural origin or of non-neural origin that secondarily involves the plexus [1]. Although several studies have assessed MRI features that may help differentiate benign peripheral nerve sheath tumours (BPNSTs) from malignant peripheral nerve sheath tumours (MPNSTs), there is none that specifically considers primary tumours of the brachial plexus. The reported morphological MRI features that are associated with MPNST include poorly defined margins [2], large size [3–7], a peripheral enhancement pattern [2, 5], peri-lesional oedema-like signal intensity (SI) [8], intra-tumoural cystic change [5, 9], an association with neurofibromatosis type 1 (NF-1) [4, 5, 9] and absence of a 'fascicular' [10, 11] or 'target' sign [9, 11–17]. However, these described MRI features have only moderate sensitivity and specificity for differentiating BPNST from MPNST [18], which has led to research in advanced MRI techniques utilising diffusion-weighted imaging (DWI) [6, 8, 9, 19, 20], diffusion tensor imaging (DTI) and tractography [21, 22] in an attempt to improve imaging differentiation.

✉ I. Pressney
ianpressney@nhs.net

[1] Department of Radiology, Royal National Orthopaedic Hospital, Brockley Hill, Stanmore, Middlesex HA7 4LP, UK

[2] Department of Radiology, Sheikh Shakhbout Medical City, Abu Dhabi, United Arab Emirates

[3] Department of Radiology, University Hospitals Plymouth NHS Trust, Plymouth, UK

However, such MRI techniques are not in routine clinical use, so there is still a reliance on accurate lesion assessment utilising conventional MRI sequences.

Murphey et al. described MPNST as having macroscopic tumour spread along the entering and exiting nerves with the epineurium and perineurium becoming thickened resulting in apparent thickening of the nerve adjacent to the tumour, rather than the expected minor tapering of the adjacent nerve documented in BPNST [23]. In the current study, the senior author observed lobular thickening of the entering nerve in a surgically proven case of supra-clavicular brachial plexus MPNST, which prompted this retrospective study of all histologically confirmed primary neural tumours arising in the brachial plexus. The MRI appearance of the entering and exiting nerve was assessed to determine if this was an additional valuable differentiating feature between BPNST and MPNST.

Materials and methods

The study was approved by the local Research and Innovation Service of the Institute of Orthopaedics under the Integrated Research Application System (IRAS) 262826, with no requirement for informed patient consent.

All patients with a confirmed histopathological diagnosis of a primary tumour of the brachial plexus were retrospectively identified from the pathology database from June 2007 to December 2019 in the setting of specialist musculoskeletal sarcoma and peripheral nerve injuries units. A total of 98 patients were identified in the preliminary search, with all diagnoses confirmed by experienced musculoskeletal pathologists on surgical resection specimens. Thirteen patients were excluded from the study, 5 tumours being of non-neural origin (1 lymphoma; 2 cases each of haemangioma and synovial sarcoma), whilst a further 7 cases were excluded (1 neurovascular hamartoma and 6 intra-neural perineuriomas). The latter were excluded due to their typical well-documented involvement of long segments of the involved nerve [24]. Therefore, only confirmed cases of schwannoma, neurofibroma and MPNST were included in the study.

Clinical data collected included age at presentation, gender and the presence of NF-1 (only 78 of the 85 patients in the study (92%) had enough clinical information available to assess this variable). Most MRI studies were obtained prior to referral ($n = 60$; 70.6%) and therefore comprised a various combination of sequences. MRI examinations were repeated at our institution as part of lesion follow-up but no MRI was repeated due to quality reasons and all presentation MRI studies were included in the study. However, the majority included at least one T1-weighted turbo spin echo (T1W TSE), T2-weighted fast spin echo (T2W FSE) and short tau inversion recovery (STIR) sequence in a combination of axial and coronal planes. Thirty-nine (45.8%) patients had intravenous contrast-enhanced MRI studies for review. The remaining patients ($n = 25$) had imaging following referral at our institution, typically a combination of coronal T1W TSE and STIR, sagittal T2W FSE, and axial proton density-weighted fast spin echo (PDW FSE) and spectral attenuated inversion recovery (SPAIR) sequences. The MRI features were independently evaluated by two consultant musculoskeletal radiologists with 8 and 5 years' experience of musculoskeletal tumour imaging who were blinded to the histological diagnosis. Lesion location (supra-clavicular, retro-clavicular or infra-clavicular) was noted. The appearance of the entering and exiting nerve was defined as being either normal, showing minor smooth tapering or lobular enlargement. A normal appearing nerve was defined as being linear in morphology and of uniform width to the margin of the lesion. Minor smooth tapering was defined as smooth expansion of the nerve towards the margin of the lesion to the nerve with no change in signal intensity (SI) of the nerve. Lobular enlargement was defined as convex swelling of the nerve at the margin of the lesion with the enlarged nerve having similar SI characteristics to the primary tumour. In addition, the presence of 'target' and 'fascicular' signs, intra-tumoural cystic change, enhancement pattern (homogeneous, heterogeneous, or peripheral) and the plexiform neurofibroma were recorded. A 'target' sign was defined as a hyperintense rim surrounding a central iso/hypointense area on T2W TSE sequences. A 'fascicular' sign was defined as multiple 'dot-like' structures with the tumour on T2W/PDW FSE or SPAIR sequences representing the nerve fascicles within the tumour. Intra-tumoural cystic change was defined as focal fluid SI. Plexiform neurofibroma was defined as a longitudinal proliferation of neural elements involving the brachial plexus. Finally, both readers suggested an MRI diagnosis of BPNST, MPNST or indeterminate based on the available MRI studies.

Statistical analysis

Inter-observer correlation was assessed using the kappa statistic for categorical variables for all MRI features, and the intra-class correlation (ICC) method for the continuous variables of patient age and maximal tumour dimension with a p value of < 0.05 taken as representing statistical significance. The associations between MRI variables and final histological diagnosis were assessed using chi-square test or Fisher's exact test when the numbers in some categories were small. Finally, sensitivity, specificity, and positive and negative predictive values (PPVs and NPV) were calculated for determining the relationship between the appearance of the entering and exiting nerve with final histological diagnosis.

Results

The final study group included 85 patients, 47 males and 38 females with a mean age of 46.7 years (range, 8–81 years), with 10 patients (11.8%) having an underlying diagnosis of NF-1. The final histological diagnoses were BPNST ($n = 73$; 85.9%) and MPNST ($n = 12$; 14.1%), the benign lesions including 66 (77.6%) schwannomas and 7 (8.2%) neurofibromas, whilst 4 (4.7%) plexiform neurofibromas were also identified. Six of 68 (91%) patients with BPNST and 4 of 10 (40%) with MPNST had NF-1. The mean age for patients with a BPNST was 47 years (range, 8–81 years) with 39 males and 34 females, compared to 44.2 years (range, 17–71 years) with 8 males and 4 females with MPNST. There was no statistical difference for gender ($p = 0.37$) or age ($p = 0.62$) between BPNST and MPNST. Regarding tumour location, 65.1% were supra-clavicular (49 BPNSTs and 7 MPNSTs) (Fig. 1), 15.1% were retro-clavicular (11 BPNSTs and 2 MPNSTs) and 19.8% were infra-clavicular (13 BPNSTs and 3 MPNSTs) (Fig. 2), there being no significant relationship between location and final diagnosis ($p = 0.64$). The mean maximal tumour dimension of BPNSTs was 3.3 cm (range, 1–11.2 cm) compared to 7.9 cm (range, 3.6–12.8 cm) for MPNSTs, this being highly significant ($p < 0.001$).

Table 1 gives details of inter-observer agreement for the 2 readers for all assessed MRI variables, the majority varying between moderate-to-good. Inter-observer correlation for the status of the entering and exiting nerves was only poor-to-fair, which was likely due to differences in agreement between a normal and tapered appearance. When these 2 categories were grouped together since they were both features suggestive of BPNST, the kappa score improved to 0.6 and 0.50 for entering and exiting nerves respectively. Results of the assessed MRI variables for reader 1 are presented in Table 2. In 5 (6.8%) cases of BPNST, the entering nerve could not be confidently visualised by reader 1, whereas the entering nerve was confidently identified in all cases of MPNST. In 7 (9.5%) cases of BPNST, the exiting nerve could not be confidently visualised by reader 1 compared to 4 (33.3%) cases for MPNST. Based on the results of reader 1, a normal or tapered (Figs. 2a and 3a) appearance of the entering nerve was seen in 55 cases of BPNST and 2 cases of MPNST, whilst a normal (Fig. 2b) or tapered (Fig. 3) appearance of the exiting nerve was seen in 62 cases of BPNST and 2 cases of MPNST. Lobular thickening of the entering nerve was seen in 13 cases of BPNST (Figs. 1 and 4) and 10 cases of MPNST. The difference in morphology of the entering nerve was statistically significant for both readers ($p < 0.001$). Similarly, lobular thickening of the exiting nerve was seen in 6 cases of BPNST compared to 6 cases of MPNST (Fig. 5), this difference again being statistically significant for both readers ($p < 0.001$). A 'target' sign (Fig. 3) was demonstrated in 12 BPNSTs compared to 0

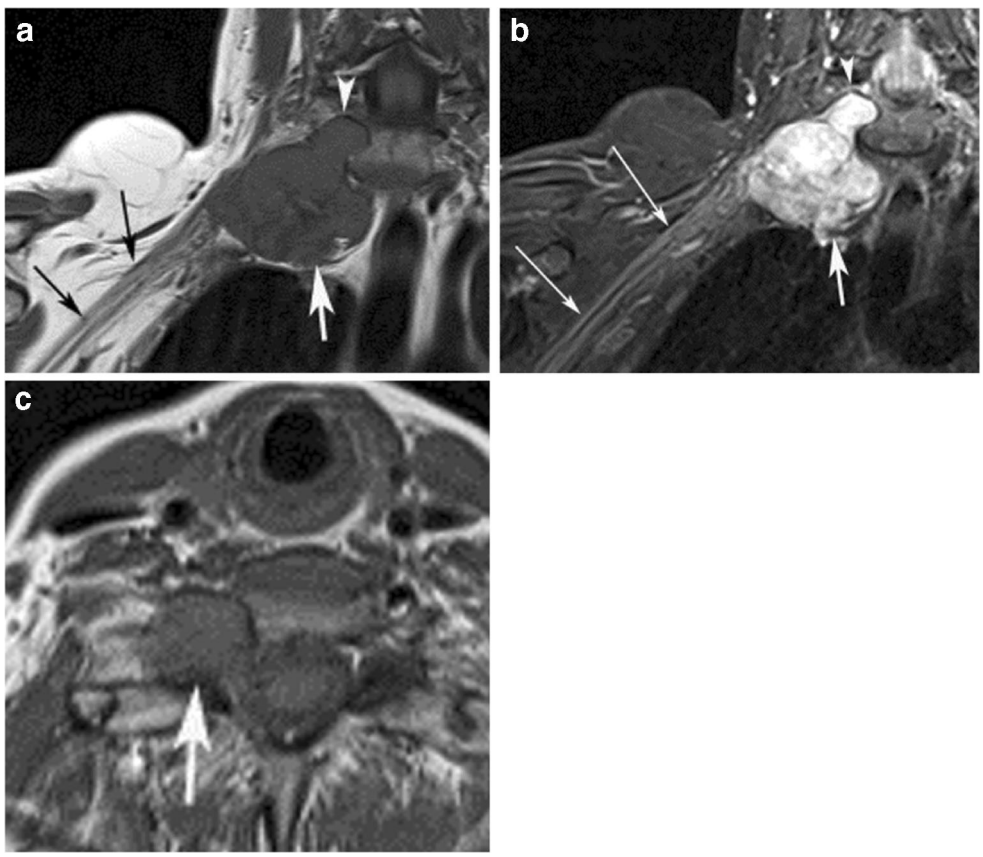

Fig. 1 A 65-year-old lady with a right supra-clavicular mass. **a** Coronal T1W TSE and **b** STIR MR images show an irregular lesion (arrows) with lobular expansion of the entering nerve (arrowheads) and a normal appearing exiting nerve (long arrows). **c** Axial T1W TSE MR image shows the expanded entering nerve (arrow) enlarging the foramen. An imaging diagnosis of MPNST was suggested, but the lesion was a schwannoma

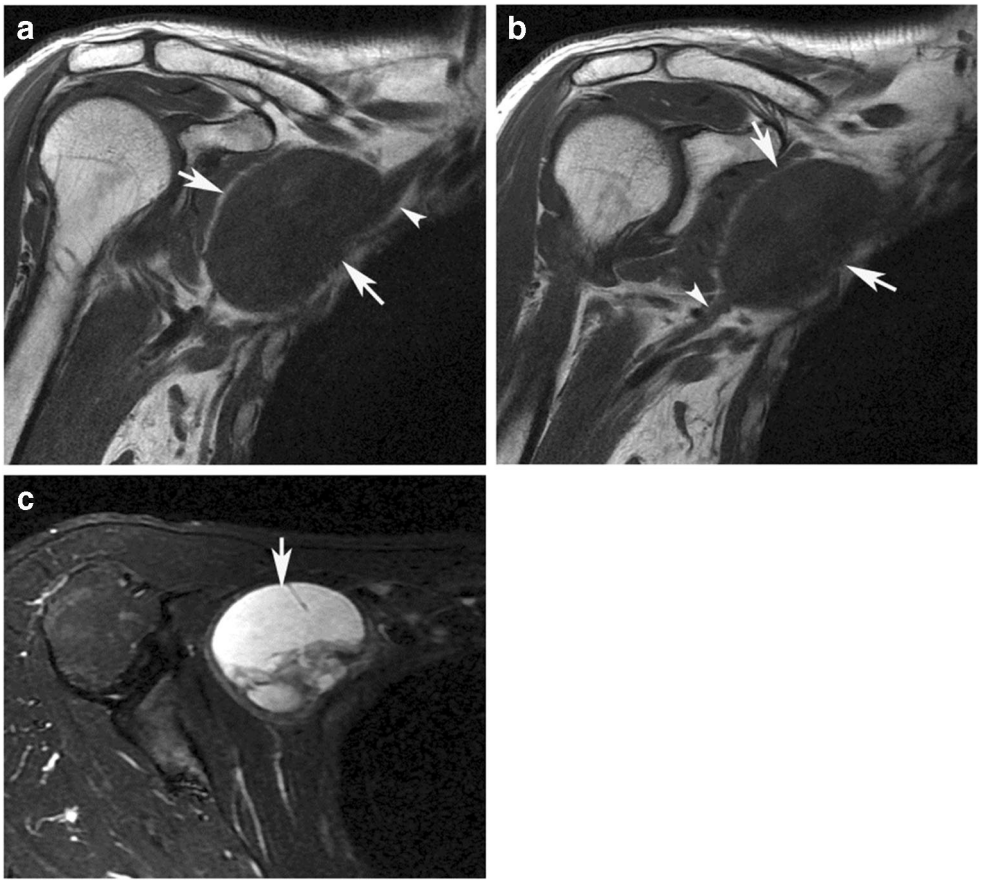

Fig. 2 A 42-year-old male with a right infra-clavicular mass. **a**, **b** Coronal T1W TSE MR images show a well-defined oval mass (arrows) with a tapered appearance to the entering nerve (arrowhead—**a**) and a normal appearance of the exiting nerve (arrowhead—**b**). **c** Axial fat-suppressed T2W FSE MR image shows extensive cystic degeneration (arrow). Resection histology confirmed a schwannoma with ancient change

MPNST ($p = 0.2$), whilst a 'fascicular' sign (Fig. 4b) was demonstrated in 8 BPNSTs compared to 0 in MPNSTs ($p = 0.59$). Intra-tumoural cystic change (Fig. 2c) was demonstrated in 12 BPNSTs compared to 2 MPNSTs ($p = 1.0$). Three BPNSTs were associated with plexiform neurofibromas compared to 1 MPNST ($p = 0.46$). Post-contrast MRI studies were available in 40 (46.5%) cases, 33 with BPNST and 7 with MPNST. Of BPNSTs, 14 showed heterogeneous enhancement, 6 showed homogenous enhancement and 13 showed peripheral enhancement, whilst for MPNSTs, 3 showed heterogeneous enhancement, 1 showed homogenous enhancement and 3 showed peripheral enhancement ($p = 0.24$).

Table 1 Inter-observer agreement of both categorical and continuous variables between readers 1 and 2

Variable	**Kappa (95% CI)**	**Kappa interpretation**
Site of lesion	0.70 (0.55, 0.86)	Good
Entering nerve status	0.33 (0.14, 0.52)	Fair
Exiting nerve status	0.11 (− 0.08, 0.30)	Poor
Target sign	0.57 (0.37, 0.78)	Moderate
Fascicular sign	0.13 (− 0.08, 0.34)	Poor
Ancient change	0.37 (0.16, 0.58)	Moderate
Enhancement	0.74 (0.50, 0.98)	Good
Plexiform NF	0.42 (0.23, 0.62)	Moderate
Imaging diagnosis	0.42 (0.28, 0.56)	Moderate
Variable	**ICC (95% CI)**	**ICC interpretation**
Maximum size*	0.91 (0.87, 0.94)	Very good

(*) Variable analysed on the log scale

There was discrepancy between the proposed MRI diagnosis of BPNST or MPNST and final histological diagnosis in 9 of 82 (11%) cases for reader 1 and 4 of 83 (4.8%) for reader 2 considering 3 and 2 indeterminate MRI diagnoses respectively. Reader 1 mis-diagnosed BPNST as MPNST in 7 cases and MPNST as BPNST in 2 cases, whilst reader 2 mis-diagnosed BPNST as MPNST in 2 cases and MPNST as BPNST in 2 cases.

When considering the entering and exiting nerve morphology as an independent diagnostic criterion, both readers had very similar results. Therefore, for simplicity, only the findings for reader 1 are presented (Table 3). When the entering or exiting nerve had a normal appearance, there was 100% sensitivity for BPNST and 100% NPV for MPNST, but specificity was low (26% for entering nerve and 30% for exiting nerve). When the entering nerve had a normal or tapered appearance, there was 83% sensitivity for BPNST and specificity rose to 81%, whilst NPV for MPNST remained high at 97%. When the exiting nerve had a normal or tapered

Table 2 Comparison of MRI features between BPNST and MPNST for reader 1. Significant findings in italics

Variable	Category	Benign, *N* (%)	Malignant, *N* (%)	*p* value
Entering nerve status	Normal	17 (100%)	0 (0%)	*< 0.001*
	Tapered	38 (95%)	2 (5%)	
	Lobular enlargement	13 (57%)	10 (44%)	
	Not identified	5 (100%)	0 (0%)	
Exiting nerve status	Normal	20 (100%)	0 (0%)	*< 0.001*
	Tapered	42 (95%)	2 (5%)	
	Lobular enlargement	6 (50%)	6 (50%)	
	Not identified	5 (56%)	4 (44%)	
Target sign	No	61 (84%)	12 (16%)	0.20
	Yes	12 (100%)	0 (0%)	
Fascicular sign	No	65 (85%)	12 (15%)	0.59
	Yes	8 (100%)	0 (0%)	
Cystic change	No	61 (86%)	10 (14%)	1.00
	Yes	12 (86%)	2 (14%)	
Enhancement pattern	Heterogeneous	14 (82%)	3 (18%)	0.24
	Peripheral	13 (93%)	1 (7%)	
	Homogeneous	6 (67%)	3 (33%)	
Plexiform NF	No	70 (87%)	11 (13%)	0.46
	Yes	3 (75%)	1 (25%)	
NF-1	No	62 (91%)	6 (9%)	*0.0059*
	Yes	6 (60%)	4 (40%)	
MRI diagnosis	BPNST	64 (97%)	2 (3%)	*< 0.001*
	Indeterminate	2 (67%)	1 (33%)	
	MPNST	7 (9%)	9 (56%)	

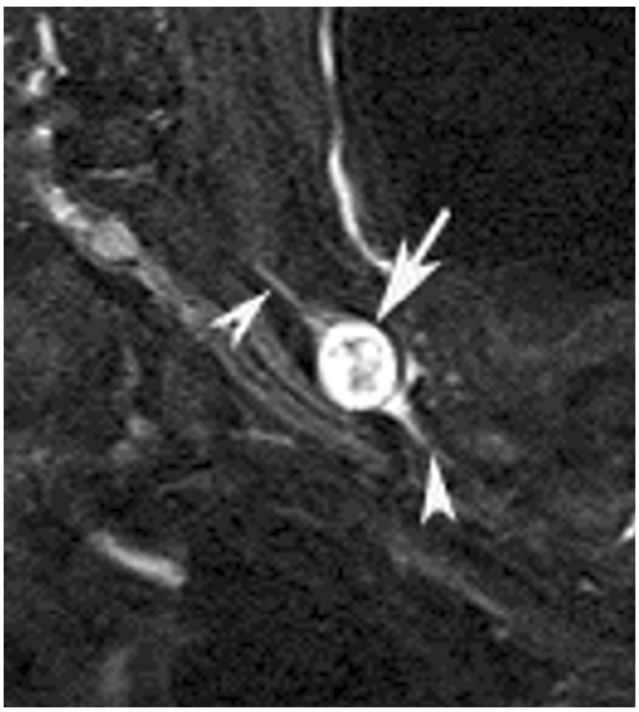

Fig. 3 A 71-year-old male with a left-sided neck mass. Coronal STIR MR image shows a target sign within the lesion (arrow) and a slightly tapered appearance to the entering and exiting nerves (arrowheads). Resection histology confirmed a schwannoma

appearance, there was 73% sensitivity for BPNST and specificity rose to 91%, whilst NPV for MPNST remained high at 97%.

Discussion

Primary tumours of the brachial plexus are uncommon, with few large series reported [19, 25, 26]. This combined group of 337 cases included 181 schwannomas, 127 neurofibromas and 29 MPNSTs [19, 25, 26], and therefore MPNST accounted for only ~9% of cases. In the current study, only 12 of 85 (14.1%) primary brachial plexus tumours were malignant. This statistic needs to be considered when reporting on MRI studies of brachial plexus tumours. In practical terms, it is of value to know whether a brachial plexus tumour is benign or malignant prior to surgery, since the management approach to BPNST and MPNST is radically different [26]. Both ultrasound and CT-guided core needle biopsy have a high diagnostic accuracy in the pre-operative assessment of PNSTs but can be associated with significant post-procedural pain [27–29]. Therefore, an accurate non-invasive clinical and imaging diagnosis of BPNST or MPNST is ideal, particularly in the brachial plexus where the anatomy is complex and percutaneous biopsy may be more challenging.

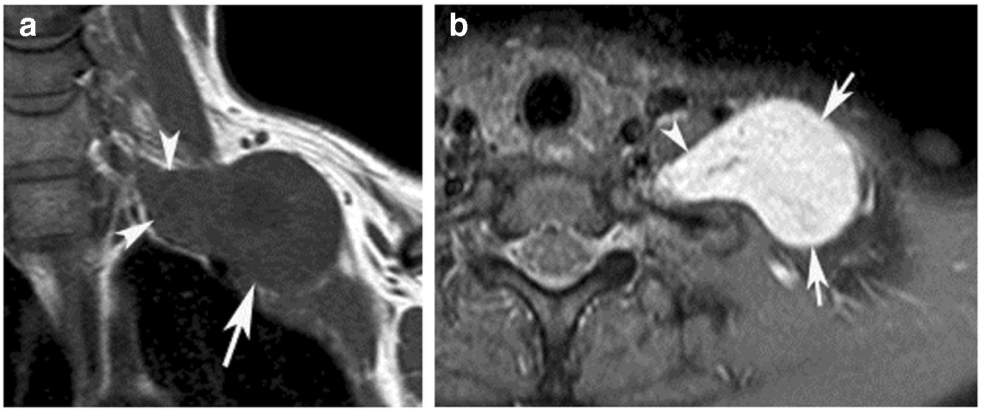

Fig. 4 A 37-year-old female with a left-sided neck mass. **a** Coronal T1W TSE and **b** axial SPAIR MR images show an oval mass (arrows) with marked lobular thickening of the entering nerve (arrowheads). The axial image also demonstrates a fascicular sign. Resection histology confirmed a schwannoma

A recent study has suggested that MRI assessing purely morphological features has only moderate accuracy with limited sensitivity and specificity for differentiating BPNST from MPNST, whilst functional techniques such as DWI and DTI may be of added value [18]. However, previous studies have not assessed the potential value of the morphological status of the entering and exiting nerves as a diagnostic criterion in relation to PNSTs arising from major nerves. The classic fusiform appearance of nerve sheath tumours with an entering and exiting nerve is well-documented for lesions arising from the major nerves including the brachial plexus [1], and is commonly demonstrated in PNSTs [23, 30, 31]. However, review of the literature shows varying incidence of continuity of the tumour with a specific nerve, termed the 'entering or exiting nerve sign'. Li et al. [3] reported that 15 of 17 (88.2%) BPNSTs and 0 of 9 MPNSTs showed continuity with a nerve, whilst Shimose et al. [14] reported continuity in 26 of 29 (89.7%) neurogenic lesions associated with major nerves compared with only 1 in 7 (14.3%) intra-

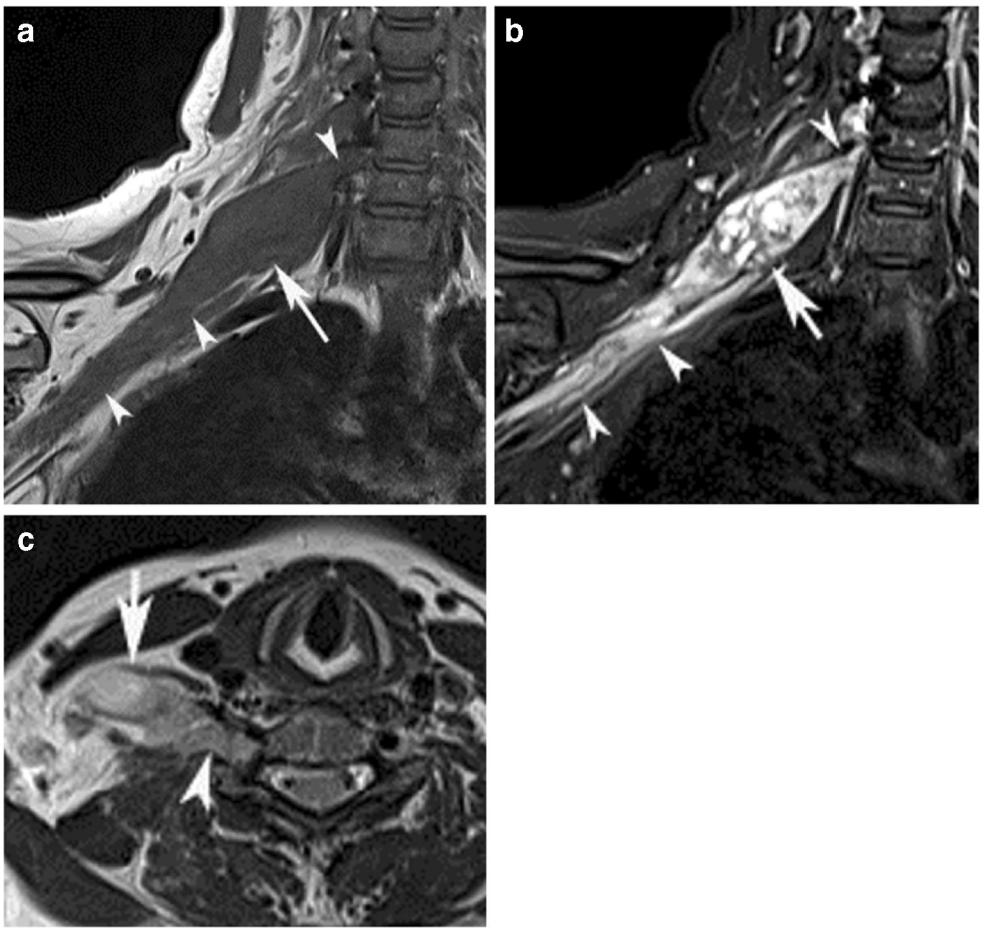

Fig. 5 A 39-year-old female with a right-sided neck mass. **a** Coronal T1W TSE and **b** STIR MR images show an elongated plexus tumour (arrows) with lobular thickening of the entering and exiting nerves (arrowheads). **c** Axial PDW FSE MR image shows the lesion (arrow) with a thickened entering nerve. Resection histology confirmed MPNST grade 2

Table 3 Sensitivity, specificity, PPV, and NPV of various combinations of entering and exiting nerve MRI appearance for distinguishing BPNST from MPNST for reader 1

Categorisation	Statistic	*n*/*N*	Value (95% CI)
Entering nerve status			
Normal vs. tapered/lobular enlargement	Sensitivity	12/12	100% (74%, 100%)
	Specificity	17/70	24% (16%, 38%)
	Positive PV	12/63	19% (10%, 31%)
	Negative PV	17/17	100% (82%, 100%)
Normal/tapered vs. lobular enlargement	Sensitivity	10/12	83% (52%, 98%)
(kappa 0.60 (0.39, 0.83))	Specificity	55/68	81% (70%, 90%)
	Positive PV	10/23	44% (23%, 66%)
	Negative PV	55/57	96% (88%, 100%)
Exiting nerve status			
Normal vs. tapered/lobular enlargement	Sensitivity	8/8	100% (63%, 100%)
	Specificity	20/68	29% (20%, 43%)
	Positive PV	8/56	14% (6%, 26%)
	Negative PV	20/20	100% (83%, 100%)
Normal/tapered vs. lobular enlargement	Sensitivity	6/8	75% (35%, 97%)
(kappa 0.50 (0.29, 0.71))	Specificity	62/68	91% (82%, 97%)
	Positive PV	6/12	50% (21%, 79%)
	Negative PV	62/64	97% (89%, 100%)

muscular nerve sheath tumours ($p < 0.01$). This is similar to the current study with > 90% BPNSTs and > 66% MPNSTs demonstrating either an entering or exiting nerve sign in the brachial plexus. Histopathologic assessment of MPNST describes macroscopic spread along the entering and/or exiting nerve epineurium and perineurium resulting in apparent thickening of the proximal and/or distal nerve [23, 32]. However, no previous study has assessed the resulting imaging appearance and its incidence. Therefore, we attempted to test the hypothesis that the MRI finding of lobular thickening of the nerve adjacent to the lesion represents the more aggressive nature of MPNST due to tumour spread along the epineurium and perineurium. For the purposes of this study, this was defined as lobular thickening of the nerve with similar SI characteristics to the primary lesion, as opposed to a completely normal calibre or smooth fusiform tapering of the adjacent nerve. The current study suggests that a normal or tapered morphology of either the entering or exiting nerves is a highly significant feature in favour of BPNST ($p < 0.001$) with both an entering and exiting 'sign' demonstrable in approximately 95% of lesions, the exiting nerve only being identifiable in 66% of MPNST compared with 93% of BPNST. Moreover, the identification of a normal appearing entering or exiting nerve was demonstrated to have 100% sensitivity for BPNST and 100% NPV for MPNST for both readers, making this a highly valuable additional morphological imaging feature in the differentiation of these two lesions. However, if only a normal appearing nerve was considered, then specificity was low at 26% for the entering nerve and 30% for the exiting nerve, whilst there were also low positive predictive values of 19% and 44% respectively. This may be due to poor to moderate inter-observer agreement for these signs which by definition may be difficult to differentiate. Therefore, by combining a normal or tapered appearance to the entering or exiting nerves, sensitivity reduced to 83% and 75% respectively but specificity increased to 81% and 91% respectively for the entering and exiting nerves. Given the low prevalence of MPNST, it would be more favourable when considering this morphology as a diagnostic tool to have a greater specificity. Grouping normal and tapered nerve morphology against lobular thickening resulted in improved specificity (now with combined sensitivity and specificity of > 1.5). Importantly, when combining the normal and tapered appearance to the entering and exiting nerves, NPV for MPNST remained very high at 97%. Therefore, when considering the morphology of the adjacent nerve as a predictor for malignancy, it may be beneficial to assess for a normal or tapered nerve against lobular thickening given the improved specificity in our study. Furthermore, the increased inter-reader reliability for grouping these features together (kappa 0.5–0.6) and not having to distinguish between a normal or tapered nerve as compared to lobular thickening (0.11–0.33) suggests that subgrouping these imaging features together has the potential for greater consistency and repeatability as a

diagnostic tool in clinical practice. This is in distinction to a previous study which documented that both BPNSTs and MPNSTs maintain a spindle shape, suggesting that the shape of a nerve sheath lesion was not a discriminating factor [3].

The current study also confirmed the significance of tumour size for differentiating BPNST and MPNST ($p = 0.004$), which agrees with several previous studies in patients with [5] and without NF-1 [3, 4, 6, 7]. The presence of a 'target sign' was not a statistically significant discriminating factor in the current study but was more frequently associated with BPNST and never seen in MPNST ($p = 0.2$). The presence of a 'fascicular sign' has been less commonly investigated but has a documented sensitivity of 100% for intra-muscular schwannomas [11]. The current study only demonstrated 8–10 cases with a 'fascicular sign', all of which were in schwannomas. Intra-tumoural cystic change was not a discriminating feature in the current study ($p = 1.0$), in contrast to reports by Wasa et al. [5] and Well et al. [9] who both reported statistically significant results for cystic change being indicative of MPNST. Similarly, the current study showed no significant difference in enhancement pattern between BPNST and MPNST, whilst previous reports have indicated that either heterogeneous enhancement [4, 15] or peripheral enhancement patterns [5] were significantly associated with MPNST.

The current study has several limitations. Most MRI studies were obtained prior to referral, resulting in a wide variation of MRI techniques. The imaging acquisition was therefore not standardised. As a result, the imaging reviewed by the readers was of satisfactory diagnostic quality to enable confident assessment of the assessed variables. The morphological assessment of the entering and exiting nerves was subjective rather than objective and showed only poor-to-fair inter-observer correlation when assessed as normal, tapered or lobular. However, by grouping the normal and tapered appearance, this resulted in a higher kappa score making the sign more reliable**.** The number of MPNSTs was relatively small, but consistent with the proportion in previous series [19, 25, 26]. All MPNSTs were histologically high-grade tumours (Trojani grade 2 or 3), and therefore there were no low-grade tumours that may have had more indeterminate or 'less aggressive' imaging features. Further studies assessing the utility of this sign should be undertaken for all PNSTs associated with major nerves, allowing the sign to be evaluated in a larger group of patients. No pathological correlation was undertaken specifically looking at the gross macroscopic and microscopic pathology of the proximal and distal aspects of the lobular nerve enlargement, which should be the subject of a further prospective study.

In conclusion, the MRI finding of a normal or tapered morphology of the entering and exiting nerves related to a primary tumour of the brachial plexus has a high sensitivity and specificity for a diagnosis of BPNST, and a very high NPV for MPNST. This emphasises that particular focus on the morphology of the entering and exiting nerves on standard MR imaging should be undertaken when reporting on nerve sheath tumours in the brachial plexus.

Acknowledgments The authors would like to acknowledge Paul Bassett for statistical support.

Compliance with ethical standards

Conflict of interest The authors declare that they have no conflict of interest.

References

1. Saifuddin A. Imaging tumours of the brachial plexus. Skelet Radiol. 2003;32:375–87.
2. Ogose A, Hotta T, Morita T, Yamamura S, Hosaka N, Kobayashi H, et al. Tumors of peripheral nerves: correlation of symptoms, clinical signs, imaging features, and histologic diagnosis. Skelet Radiol. 1999;28:183–8.
3. Li CS, Huang GS, Wu HD, Chen WT, Shih LS, Lii JM, et al. Differentiation of soft tissue benign and malignant peripheral nerve sheath tumors with magnetic resonance imaging. Clin Imaging. 2008;32:121–7.
4. Matsumine A, Kusuzaki K, Nakamura T, Nakazora S, Niimi R, Matsubara T, et al. Differentiation between neurofibromas and malignant peripheral nerve sheath tumors in neurofibromatosis 1 evaluated by MRI. J Cancer Res Clin Oncol. 2009;135:891–900.
5. Wasa J, et al. MRI features in the differentiation of malignant peripheral nerve sheath tumors and neurofibromas. AJR. 2010;194:1568–74.
6. Demehri S, Belzberg A, Blakeley J, Fayad LM. Conventional and functional MR imaging of peripheral nerve sheath tumors: initial experience. AJNR Am J Neuroradiol. 2014;35(8):1615–20.
7. Karsy M, Guan J, Ravindra VM, Stilwill S, Mahan MA. Diagnostic quality of magnetic resonance imaging interpretation for peripheral nerve sheath tumors: can malignancy be determined? J Neurol Surg A Cent Eur Neurosurg. 2016;77(6):495–504.
8. Soldatos T, Fisher S, Karri S, Ramzi A, Sharma R, Chhabra A. Advanced MRI imaging of peripheral nerve sheath tumors including diffusion imaging. Semin Musculoskelet Radiol. 2015;19:179–90.
9. Well L, Salamon J, Kaul MG, et al. Differentiation of peripheral nerve sheath tumors in patients with neurofibromatosis type 1 using diffusion-weighted magnetic resonance imaging. Neuro-Oncology. 2019;21(4):508–16.
10. Wu JS, Hochman MG. Soft-tissue tumors and tumorlike lesions: a systematic imaging approach. Radiology. 2009;253:297–316.
11. Salunke AA, Chen Y, Tan JH, et al. Intramuscular schwannoma: clinical and magnetic resonance imaging features. Singap Med J. 2015;56(10):555–7.
12. Bhargava R, Parham DM, Lasater OE, et al. MR imaging differentiation of benign and malignant peripheral nerve sheath tumors: use of the target sign. Pediatr Radiol. 1997;27:124–9.

13. Varma DG, Moulopoulos A, Sara AS, et al. MR imaging of extracranial nerve sheath tumors. J Comput Assist Tomogr. 1992;16(3):448–53.
14. Shimose S, Sugita T, Kubo T, et al. Major-nerve schwannomas versus intramuscular schwannomas. Acta Radiol. 2007;48:672–7.
15. Ahlawat S, Fayad LM. Imaging cellularity in benign and malignant peripheral nerve sheath tumors: utility of the "target sign" by diffusion weighted imaging. Eur J Radiol. 2018;102:195–201.
16. Koga H, Matsumoto S, Manabe J, Tanizawa T, Kawaguchi N. Definition of the target sign and its use for the diagnosis of schwannomas. Clin Orthop Relat Res. 2007;464:224–9.
17. Zhang Z, Deng L, Ding L, Meng Q. MR imaging differentiation of malignant soft tissue tumors from peripheral schwannomas with large size and heterogeneous signal intensity. Eur J Radiol. 2015;84(5):940–6.
18. Mazal AT, Ashikyan O, Cheng J, Le LQ, Chhabra A. Diffusion-weighted imaging and diffusion tensor imaging as adjuncts to conventional MRI for the diagnosis and management of peripheral nerve sheath tumors: current perspectives and future directions. Eur Radiol. 2019;29(8):4123–32.
19. Kim DH, Murovic JA, Tiel RL, Moes G, Kline DG. A series of 397 peripheral neural sheath tumors: 30-year experience at Louisiana State University Health Sciences Center. J Neurosurg. 2005;102(2):246–55.
20. Ahlawat S, Blakeley JO, Rodriguez FJ, Fayad LM. Imaging biomarkers for malignant peripheral nerve sheath tumors in neurofibromatosis type 1 [published correction appears in Neurology. 2020 Mar 17;94(11):504]. Neurology. 2019;93(11):e1076–84.
21. Schmidt M, Kasprian G, Amann G, Duscher D, Aszmann OC. Diffusion tensor tractography for the surgical management of peripheral nerve sheath tumors. Neurosurg Focus. 2015;39(3):E17.
22. Chhabra A, Thakkar RS, Andreisek G, et al. Anatomic MR imaging and functional diffusion tensor imaging of peripheral nerve tumors and tumorlike conditions. AJNR Am J Neuroradiol. 2013;34(4):8.
23. Murphey MD, Smith WS, Smith SE, Kransdorf MJ, Temple HT. Imaging of musculoskeletal neurogenic tumors: radiologic-pathologic correlation 1. Radiographics. 1999;19:1253–80.
24. Mauermann ML, Amrami KK, Kuntz NL, et al. Longitudinal study of intraneural perineurioma- a benign, focal hypertrophic neuropathy of youth. Brain. 2009;132:2265–76.
25. Lusk MD, Kline DG, Garcia CA. Tumors of the brachial plexus. Neurosurgery. 1987;21(4):439–53.
26. Jia X, Yang J, Chen L, Yu C, Kondo T. Primary brachial plexus tumors: clinical experiences of 143 cases. Clin Neurol Neurosurg. 2016;148:91–5.
27. Brahmi M, Thiesse P, Ranchere D, et al. Diagnostic accuracy of PET/CT-guided percutaneous biopsies for malignant peripheral nerve sheath tumors in neurofibromatosis type 1 patients. PLoS One. 2015;10(10):e0138386 Published 2015 Oct 7.
28. Pianta M, Chock E, Schlicht S, McCombe D. Accuracy and complications of CT-guided core needle biopsy of peripheral nerve sheath tumours. Skelet Radiol. 2015;44(9):1341–9.
29. Tøttrup M, Eriksen JD, Hellfritzsch MB, Sørensen FB, Baad-Hansen T. Diagnostic accuracy of ultrasound-guided core biopsy of peripheral nerve sheath tumors. J Clin Ultrasound. 2020;48(3):134–8.
30. Chee DW, Peh WC, Shek TW. Pictorial essay: imaging of peripheral nerve sheath tumours. Can Assoc Radiol J. 2011;62(3):176–82.
31. Kakkar C, Shetty CM, Koteshwara P, Bajpai S. Telltale signs of peripheral neurogenic tumors on magnetic resonance imaging. Indian J Radiol Imaging. 2015;25(4):453–8.
32. WHO Classification of Tumours Editorial Board. WHO Classification of Tumours of Soft Tissue and Bone. 5th ed. Lyon, France: IARC Press; 2020.